International Journal of Nanomedicine

Dovepress
Taylor & Francis Group

Open Access Full Text Article

ORIGINAL RESEARCH

Bone Marrow Mesenchymal Stem Cells-Derived Exosomes Inhibit Apoptosis of Pulmonary Microvascular Endothelial Cells in COPD Mice Through miR-30b/Wnt5a Pathway

Qing Song[1–4], Aiyuan Zhou[5], Wei Cheng[1–4], Yiyang Zhao[6], Cong Liu[1–4], Yuqin Zeng[1–4], Ling Lin[1–4], Zijing Zhou[1–4], Yating Peng[1–4], Ping Chen[1–4]

[1]Department of Respiratory and Critical Care Medicine, the Second Xiangya Hospital, Central South University, Changsha, Hunan, 410011, People's Republic of China; [2]Clinical Medical Research Center for Pulmonary and Critical Care Medicine in Hunan Province, Changsha, 410011, People's Republic of China; [3]Diagnosis and Treatment Center of Respiratory Disease, Central South University, Changsha, Hunan, 410011, People's Republic of China; [4]Research Unit of Respiratory Disease, Central South University, Changsha, Hunan, 410011, People's Republic of China; [5]Department of Respiratory and Critical Care Medicine, the Xiangya Hospital of Central South University, Changsha, Hunan, 410011, People's Republic of China; [6]Ultrasound Imaging Department, Xiangya Hospital of Central South University, Changsha, Hunan, 410083, People's Republic of China

Correspondence: Ping Chen, Department of Respiratory and Critical Care Medicine, the Second Xiangya Hospital, Central South University, Renmin Middle Road, Changsha, Hunan, 410011, People's Republic of China, Tel 13873115563, Email pingchen0731@csu.edu.cn

Background: Bone marrow mesenchymal stem cells (BMSCs)-derived exosomes are rich in a variety of active substances, including microRNA (miR) and have shown powerful therapeutic effects to ameliorate cell injury and diseases. However, the role of BMSCs-derived exosomes on chronic obstructive pulmonary disease (COPD) has been poorly studied. In addition, pulmonary microvascular endothelial cells (PMVECs) apoptosis contributes to the onset of COPD. Inhibition of PMVECs apoptosis can reverse COPD changes. Therefore, the aim of this study was to explore the role of BMSCs-derived exosomes in the apoptosis of PMVECs in COPD and to investigate the potential mechanisms.

Methods: We isolated and characterized normal mouse BMSCs-derived exosomes and PMVECs. We performed miR sequencing of BMSCs-derived exosomes. We transfected PMVECs with the miR-30b mimic and Wnt5a overexpression plasmid to assess the underlying mechanisms. Cigarette smoke extract (CSE)-induced COPD mice were treated with exosomes and HBLV-mmu-miR-30b via intratracheal instillation. Finally, we determined the expression of miR-30b and Wnt5a in tissues from patients with COPD.

Results: BMSCs-derived exosomes could significantly reduce apoptosis of CSE-induced PMVECs and increase the expression of miR-30b ($p<0.05$). Based on miR sequencing, miR-30b was highly enriched in BMSCs-derived exosomes. The knockdown of miR-30b in BMSCs-derived exosomes could increase the apoptosis of CSE-induced PMVECs ($p<0.05$). miR-30b overexpression significantly reduced apoptosis and repressed Wnt5a protein expression in CSE-induced PMVECs ($p<0.05$). Furthermore, Wnt5a overexpression reversed the anti-apoptotic effect of miR-30b on CSE-induced PMVECs ($p<0.05$). In addition, compared with the COPD group, treatment with BMSCs-derived exosomes and miR-30b overexpression could alleviate emphysema changes, decrease the mean linear intercept and alveolar destructive index, reduce apoptosis, increase the expression of miR-30b, and decrease the expression of Wnt5a in lung tissue ($p<0.05$). Finally, miR-30b expression was decreased in patients with COPD, while Wnt5a expression was increased in these patients ($p<0.05$).

Conclusion: BMSCs-derived exosomes could improve the damage of COPD perhaps by delivering miR-30b. miR-30b could reduce apoptosis of CSE-induced PMVECs by targeting Wnt5a.

Keywords: chronic obstructive pulmonary disease, bone marrow mesenchymal stem cells, exosomes, miR-30b, Wnt5a

Introduction

Chronic obstructive pulmonary disease (COPD) is one of the most serious chronic respiratory diseases that can be prevented and treated. As the disease progresses, patients' quality of life declines sharply, leading to heavy social and

Received: 15 July 2024
Accepted: 14 January 2025
Published: 30 January 2025

Graphical Abstract

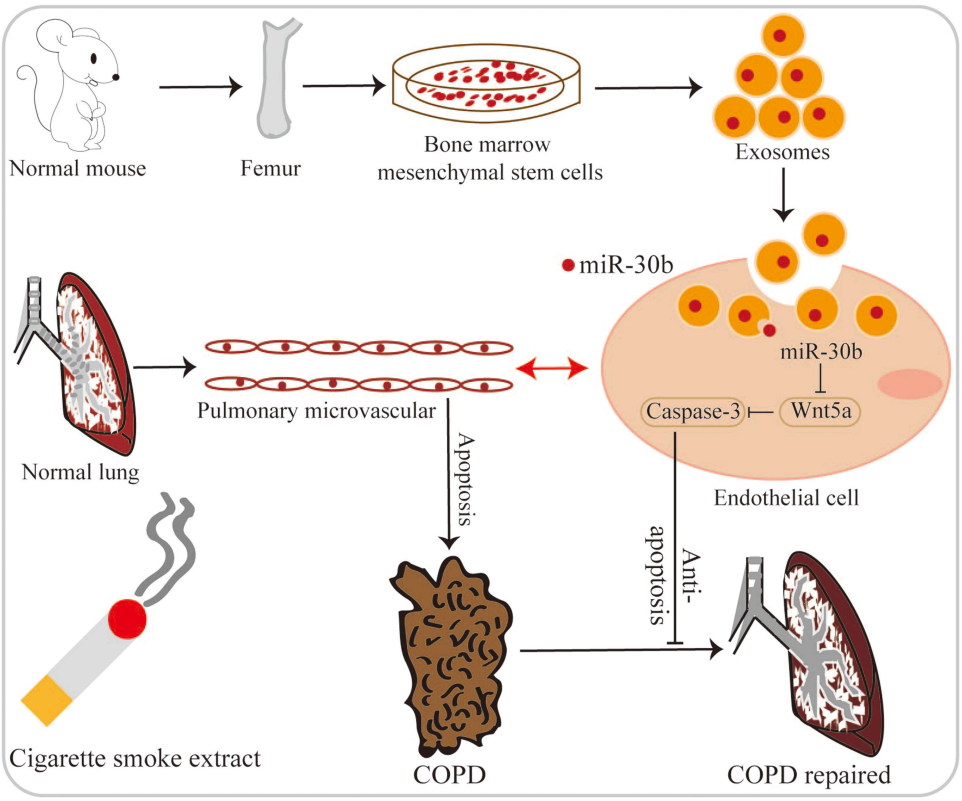

economic burden.[1,2] Currently, pharmacological therapy for COPD including bronchodilators, antimuscarinic drugs, methylxanthines, anti-inflammatory agents, oral glucocorticoids, and inhaled corticosteroids is used to reduce the symptoms and the frequency of exacerbations, and to improve exercise tolerance and the health status. However, current pharmacotherapy cannot restore the damage to alveolar and pulmonary blood vessels structure in patients with COPD.[3] Therefore, it is extremely urgent to find an effective treatment for COPD.

Smoking is the most significant risk factor for COPD: It can increase oxidative stress and apoptosis to promote cell death.[4] Studies have shown that apoptosis of pulmonary microvascular endothelial cells (PMVECs) participates in the development of COPD. Inhibition of this apoptosis can reverse or partially reverse impaired lung function and emphysema in mouse.[5–7] It is possible that inhibiting the apoptosis of cigarette smoke extract (CSE)-induced PMVECs may become an effective treatment for COPD.

Bone marrow mesenchymal stem cells (BMSCs) are adult stem cells that can differentiate into endothelial cells and fibroblasts to help repair tissue damage.[8] Exosomes are extracellular vesicles with a size range of 40 to 160 nm (average ~100 nm) in diameter with an endosomal origin. Exosomes can contain many cellular constituents, including DNA, RNA, lipids, metabolites, and cytosolic and cell-surface proteins. Exosomes are associated with immune responses, cardiovascular diseases, and cancer progression. Proteins, DNA, and RNA delivered by exosomes into recipient cells effectively alter their biological response.[9] In addition, exosomes play an important role in the development of lung disease including COPD, asthma, lung cancer, and pulmonary fibrosis.[10] MicroRNAs (miRs) are a type of non-coding RNA with a length of 22–25 nucleotide that have regulatory effects.[11] miRs also play an important role in lung disease.[12] Park et al[13] found that miR-6238 is a novel regulator of pulmonary inflammation and a putative biomarker that distinguishes particulate matter induced acute lung injury from endotoxin-mediated acute lung injury.

Wnt5a is a member of the non-classical Wnt signaling pathway, which is involved in inflammation, proliferation, apoptosis, and differentiation. Functionally, mature Wnt5a has the ability to reverse the canonical Wnt-driven alveolar epithelial cell wound healing in vitro.[14] In addition, Wnt5a can promote neoplastic transformation and small cell lung cancer cell proliferation, whereas Wnt5a deficiency inhibits small cell lung cancer development.[15] However, the role of Wnt5a in COPD has not been fully elucidated.

Therefore, the aim of this study was to explore the role of BMSCs-derived exosomes in the apoptosis of PMVECs in COPD and to investigate the potential mechanisms.

Materials and Methods

Isolation and Culture of BMSCs

We obtained six-week-old male C57BL/6J mice from the SJA Lab Animals corporation (Hunan, China) and isolated BMSCs by using the whole bone marrow adherent method described previously.[16] Briefly, the mice were sacrificed by cervical dislocation. The femur and tibia were isolated in a sterile manner and the metaphysis was removed to expose the marrow cavity. Low-glucose Dulbecco's Modified Eagle Medium (DMEM; 8122386, Gibco, USA) supplemented with 10% fetal bovine serum (FBS; 10100147, Gibco, USA) was used to rinse the contents of the marrow cavity into a sterile petri dish (Nest, 704202). The liquid was pipetted into a single cell suspension and filtered with a 100 μm filter. Next, the single cell suspension was subjected to centrifugation at 1000 rpm for 10 minutes at room temperature. Finally, the BMSCs were incubated at 37°C with 95% air and 5% CO_2 and labeled as passage 1 (P1). The BMSCs were identified by flow cytometry analysis for the surface markers, including CD11b (11–0112-82, eBioscience, USA), CD29 (11–0291-80, eBioscience, USA), CD34 (11–0341-82, eBioscience, USA), CD44 (11–0451-81, eBioscience, USA), CD45 (11–0451-82, eBioscience, USA), CD73 (127219, Biolegend, USA), and CD105 (53–1051-82, eBioscience, USA). In addition, the BMSCs were identified by osteogenic differentiation, adipogenic differentiation, and chondrogenic differentiation.

This study was approved by the Ethics Committee of the Second Xiangya Hospital of Central South University (Number: 2022200) (Hunan, China) and the animal experimental procedures are in accordance with the provisions of the "Experimental Animal Care and Use Guide".

Extraction and Identification of BMSCs-Derived Exosomes

The BMSCs from P3-P6 were selected for exosomes extraction. Exosomes were isolated by differential centrifugation as described previously with some modifications.[17] Briefly, culture supernatant of BMSCs was collected and then centrifuged at 300 *g* for 10 min at 4°C, at 2000 *g* for 10 min at 4°C, and at 12000 *g* for 45 min at 4°C. Next, the BMSCs supernatant was filtered through a 0.22 μm filter. The BMSCs supernatant was centrifuged two times at 140000 *g* for 70 min at 4°C to obtain exosomes (Beckman Coulter, USA). Finally, the exosomes were resuspended in phosphate buffered solution (PBS) and stored at −80°C.

Western blot was used to identify the surface markers of exosomes, including CD9 (ab92726, Abcam, USA), CD63 (ab231975, Abcam, USA), CD81 (ab109201, Abcam, USA), TSG101 (ab125011, Abcam, USA), and calnexin (ab22595, Abcam, USA). Nanoparticle tracking analysis was used to determine the size distribution and concentration of the exosomes with a ZetaView particle tracker (Flow NanoAnal, China). Transmission electron microscopy was performed to observe the morphology of the exosomes (HT-7800, HITACHI).

miR Sequencing

First, total RNA was extracted from BMSCs exosomes by using TRIzol reagent (15596026, Invitrogen, USA). The quality and integrity of the total RNA were assessed with an Agilent 2100 Bioanalyzer (Agilent Technologies, USA). Next, RNA was ligated with 5′ and 3′ adapters, followed by complementary DNA (cDNA) synthesis using adaptor-specific primers. Following polymerase chain reaction amplification, the RNA libraries underwent gel purification, and the quality of the libraries was evaluated. Subsequently, miR sequencing was performed on the DNBSEQ platform (BGI, China).

Study Participants

We obtained lung tissues from eleven COPD patients and seventeen controls participants undergoing lung resection due to lung cancer in the Second Xiangya Hospital's Cardiothoracic Surgery Department (Hunan, China). The basic demographic data was shown in Supplement Table 1. The diagnosis of COPD complies with GOLD 2017 guideline,[3] individuals with significant heart and other lung diseases including pulmonary fibrosis, asthma, pneumonia, and bronchiectasis were excluded.

This study was conducted following the principles of the Declaration of Helsinki and received ethical approval from the Ethics Committee of the Second Xiangya Hospital of Central South University (Number: Z0208-01). Informed consent was obtained from all participating patients.

Preparation of CSE

The CSE preparation protocol has been optimized based on previous descriptions.[18] First, we burned five cigarettes (Furong, Changde Cigarette Company, China) and bubbled the smoke with 10 mL of PBS. We extracted 35 mL of smoke every 15 seconds. Afterwards, the obtained CSE was filtered using a 0.22 μm filter to obtain a concentration of 100% CSE for the animal experiments.

In terms of in vitro study, only half a cigarette was burned, and the following steps are similar to above description. 100% CSE was diluted to a concentration of 1%, 2.5%, and 4% for the subsequent cell experiments.

Animal Model

Six-week-old male C57BL/6J mice were purchased from the SJA Lab Animals Corporation (Hunan, China). All mice were kept in a clean room in the experimental animal center of the Second Xiangya Hospital. After 1 week of acclimatization to the laboratory conditions, the mice were randomly divided into five groups (eight mice each group): the control group, the COPD group, the COPD + miR-30b negative control (COPD + miR-NC) group, the COPD + miR-30b overexpression (COPD + miR-OV) group, and the COPD + exosomes (COPD + Ex) group. To establish the COPD model, the mice were injected intraperitoneally with CSE following a previously described method.[18] First, the mice in the COPD, COPD + miR-NC, COPD + miR-OV, and COPD + Ex groups were given an intraperitoneal injection of CSE (0.01 mL/g body weight) on days 1, 11, 23, and 32, while the control group was given an intraperitoneal injection of PBS at the same times and with the same volume. On day 28, all mice were anesthetized with 1% sodium pentobarbital (50 mg/kg body weight). The COPD + Ex group was given an intratracheal instillation of BMSCs-derived exosomes (6.35×10^8 particles/50 μL).[19] The COPD + miR-NC group was given an intratracheal instillation of HBLV-ZsGreen-PURO negative control. The COPD + miR-OV group was given an intratracheal instillation of HBLV-mmu-miR-30b–ZsGreen-PURO to overexpress miR-30b (3×10^7 TU/50 μL/mouse, Hanbio Biotechnology Co. Ltd., Shanghai, China). Finally, the control and COPD groups were treated with same volume of PBS. On day 35, all mice were sacrificed by cervical dislocation. The right lung was rapidly frozen in liquid nitrogen and stored for subsequent protein and RNA extraction. The left lung was fixed in 4% paraformaldehyde for histology.

Histomorphology of Lung Tissue

The left lung was fixed in 4% paraformaldehyde for 24 h in a cold room. Next, the lung tissue was embedded in paraffin and then cut into 4 μm sections. Finally, the sections were stained with hematoxylin-eosin (HE) (H3136, Sigma, USA). We measured mean linear intercept (MLI) and the destructive index (DI) as described previously.[18,20] The MLI was measured by dividing the length of a line drawn across the lung section by a total number of intercepts counted within this line (100× magnification); a total of 36 lines were drawn and measured for each mouse. The DI was calculated by dividing the defined destructive alveoli by the total number of alveoli counted; it is presented as percentage of the destructive alveoli relative to the total alveoli. A destructive alveolus had at least one of the following abnormalities: alveolar wall defects; obviously abnormal morphology; intraluminal parenchymal rags in alveolar ducts; and typical emphysematous changes (200× magnification).

Immunohistochemistry

Lung tissue from mice and patients was fixed in 4% paraformaldehyde for 24 h and embedded in paraffin. Then, 4 μm sections were cut and used for staining. Initially, the sections were subjected to antigen retrieval in citrate buffer for 10 min in a microwave and then incubated in 0.3% hydrogen peroxide to block endogenous peroxidase activity. Next, the sections were incubated with anti-Wnt5a (BA2839, BOSTER, China, 1:100) at 4°C overnight. After this incubation, the sections were washed and incubated with a secondary antibody for 30 min. Finally, diaminobenzidine was added and hematoxylin was applied for counterstaining. The protein expression level was scored based on the staining intensity using Image J software 1.8.0 (National Institutes of Health, Bethesda, MD, USA) as follows: 0, no staining; 1, weak staining; 2, moderate staining; and 3, strong staining. The percentage of staining area was classified as: 0 (0%), 1 (1–10%), 2 (11–50%), and 3 (51–100%). The staining index was calculated as the proportion of positive cells and the staining intensity score. Each section collected three different representative nonoverlapping fields for analysis.[21]

Apoptosis in Lung Tissue

Apoptosis was identified by double staining: terminal deoxynucleotidyl transferase-mediated dUTP nick end labelling (TUNEL) (G1501, Servicebio, China) and CD31 labeling (SAF005, AIFang Biological, China), following the manufacturer's instructions. Briefly, lung sections were permeabilized with proteinase K (G1205, Servicebio) and the membrane was broken. Next, the reaction solution was added to the lung tissues and 4′,6-diamidino-2′-phenylindole (DAPI) (G1012, Servicebio, China) was applied to counterstain the nuclei. A microscope (Olympus, Japan) was used to assess the fluorescence of sections.

Isolation and Culture of PMVECs

PMVECs were sorted by magnetic beads.[21] Briefly, mice lung tissue was collected under sterile conditions. Then, the lung tissue was digested with type I collagenase solution (V900891, Sigma, USA) for 45 min at 37°C, centrifuged, and filtered with 100 μm and 40 μm cell mesh. Next, microbeads with mouse CD31 (130–097-418, Miltenyi, Germany) were added and the mixture was incubated for 15 min at 4°C. Finally, the cells were passed through an LS column (130–042-401, Miltenyi, Germany) and then centrifuged to obtain PMVECs. These cells were grown in 5% CO_2 at 37°C with a specific pulmonary vascular endothelial cell medium (1001, Sciencell, USA).

Identification of PMVECs

The von Willebrand factor (vWF) was used to identify the purity of PMVECs. Briefly, cells were blocked with 10% bovine serum albumin, and then incubated with a vWF antibody (SA00006-4, Proteintech, USA) for 12 h at 4°C. Incubate the section with a secondary antibody for 1 h and then stained with DAPI (G1012, Servicebio, China). Finally, the cells were mounted with Fluoromount-G (0100–01, SourthernBiotech, USA) and viewed under a fluorescence microscope.

Cell Transfection and Interference

PMVECs were seeded into 6-well plates until they reached 70–80% confluence. Lipofectamine 3000 (L3000015, Invitrogen, USA) was used to transfect PMVECs with the miR-30b mimic (to achieve miR-30b overexpression), the NC mimic (negative control), the Wnt5a overexpression plasmid (pEXP-RB-Mam-EGFP2-Wnt5a, pEXP-Wnt5a), and empty plasmid (pEXP-RB-Mam-EGFP2, pEXP-empty) (RiboBio Corporation, Guangzhou, China). Twenty-four hours after transfection, PMVECs were treated with 2.5% CSE for 24 h.

The BMSCs were seeded and when the density reached 50–60%, an MOI value of 30 was used, knockdown of lentivirus miR-30b (HBLV-mmu-miR-30b-sponge-ZsGreen-PURO, miR-sponge) and lentivirus negative control (HBLV-ZsGreen-PURO, NC) (Hanbio Biotechnology Co. Ltd., Shanghai, China) were added; the solution was changed after 16 h. The culture supernatant of BMSCs was collected to obtain exosomes for subsequent experiments.

Western Blot

The protocol was similar to what has been published previously.[18] In brief, total protein from the cells or lung tissue was extracted, and the protein concentration was determined. After protein separation and transfer to a membrane, the membrane was incubated with the appropriate primary antibody for 24 h at 4°C: Bcl-2 (#3498, CST, USA, 1:1000), Bax (14796, CST, USA, 1:1000), cleaved caspase-3 (#9661, CST, USA, 1:1000), GAPDH (10494-1-AP, Proteintech, USA, 1:5000), Wnt5a (BA2839, Boster, China, 1:1000), and β-actin (AC038, ABclonal, China, 1:10,000). After incubation, the membrane was washed and incubated with the appropriate secondary antibody for 1 h at room temperature: goat anti-rabbit IgG conjugated to horseradish peroxidase (HRP) (SA00001-2, Proteintech, USA, 1:10000) or goat anti-mouse IgG conjugated to HRP (SA00001-1, Proteintech, USA, 1:10,000). Finally, the protein bands were detected using enhanced chemiluminescence substrate (GE2301, GENVIEW).

Reverse Transcription Quantitative Polymerase Chain Reaction (RT-qPCR)

Total RNA was extracted using the TRIzol reagent (15596026, Invitrogen, USA). After determining the RNA concentration, it was reverse transcribed using the RevertAid First Strand cDNA Synthesis Kit (K1622, Thermo, USA). Then, RT-qPCR was performed with SYBR green master mix (11184ES08, Yeasen, China) following the manufacturer's instructions. The stem-loop method was used to reverse transcribe miRs. The primers of miR-30b (Lot 2131), mmu-let -7f-5p (Lot U0413), mmu-let-7a-5p (Lot Q0111), mmu-let-7c-5p (Lot R0815), mmu-let-7d-5p (Lot R0506), and U6 (Lot Q1124) were designed and constructed by RiboBio Corporation (Guangzhou, China). Each reaction was run in triplicate.

Flow Cytometry Analysis

Annexin V and propidium iodide (PI) staining (2324718, Invitrogen, USA) were used to analyze PMVECs apoptosis. After the PMVECs were washed and centrifuged, they were suspended in 200 μL of binding buffer and incubated with Annexin V for 15 min. Finally, the cells were incubated with PI. To set gates and to establish appropriate compensation settings, cells were stained with Annexin V alone, PI alone or neither reagent (blank). In this study, apoptotic PMVECs were positive for Annexin V and negative for PI (Quadrants 3, Q3).

Luciferase Assay

First, wild-type and mutant Wnt5a (Wnt5a-WT and Wnt5a-MT, respectively) plasmids were constructed (Bio Technology Company, China). Then, the mmu-miR-30b mimic or the NC mimic, and the Wnt5a-WT or Wnt5a-MT plasmid (1 μg/well in 6 well plates) were transfected into PMVECs by using Lipofectamine 3000 (L3000015, Invitrogen, USA). Twenty-four hours after transfection, firefly and Renilla luciferase activities were measured by using the dual-luciferase assay kit (KGAF040, Keygen Company, Jiangsu, China) following the manufacturer's instructions. The normalized luciferase activity is expressed as the ratio of firefly luciferase to Renilla luciferase units.

Statistical Analysis

Statistical analysis was performed using SPSS Statistics Version 26.0 (IBM Corp., USA). Continuous variables with a normal distribution and homogeneous variances were expressed as mean ± standard deviation and were compared with the independent-samples *t*-test or analysis of variance. Least Significant Difference -*t* test was used for pairwise comparison between groups if continuous variables with a normal distribution and homogeneous variances. Continuous variables with a non-normal distribution or an uneven variance were expressed as interquartile range (IQR) and were compared with non-parametric methods. Kruskal–Wallis test was used for pairwise comparison between groups if continuous variables with a non-normal distribution or an uneven variance. A p-value < 0.05 was considered to be statistically significant.

Results

Isolation and Identification of BMSCs and Exosomes

Figure 1A and B shows the morphology of BMSCs which were adherent growth. When induced to undergo osteogenic differentiation, there was a large amount of dark red bone tissue (Figure 1C). There was a large number of brown-yellow adipocytes after adipogenic differentiation (Figure 1D). In addition, there was a large number of blue cartilage cells after chondrogenic differentiation (Figure 1E). We also identified BMSCs by using flow cytometry analysis; of the cells, 97.64% were positive for CD29, 99.16% were positive for CD44, 99.26% were positive for CD73, 94.34% were positive for CD105, 0.45% were positive for CD34, 3.89% were positive for CD45, and 2.82% were positive for CD11b (Figure 1F). These results indicated that most of the cells were indeed BMSCs.

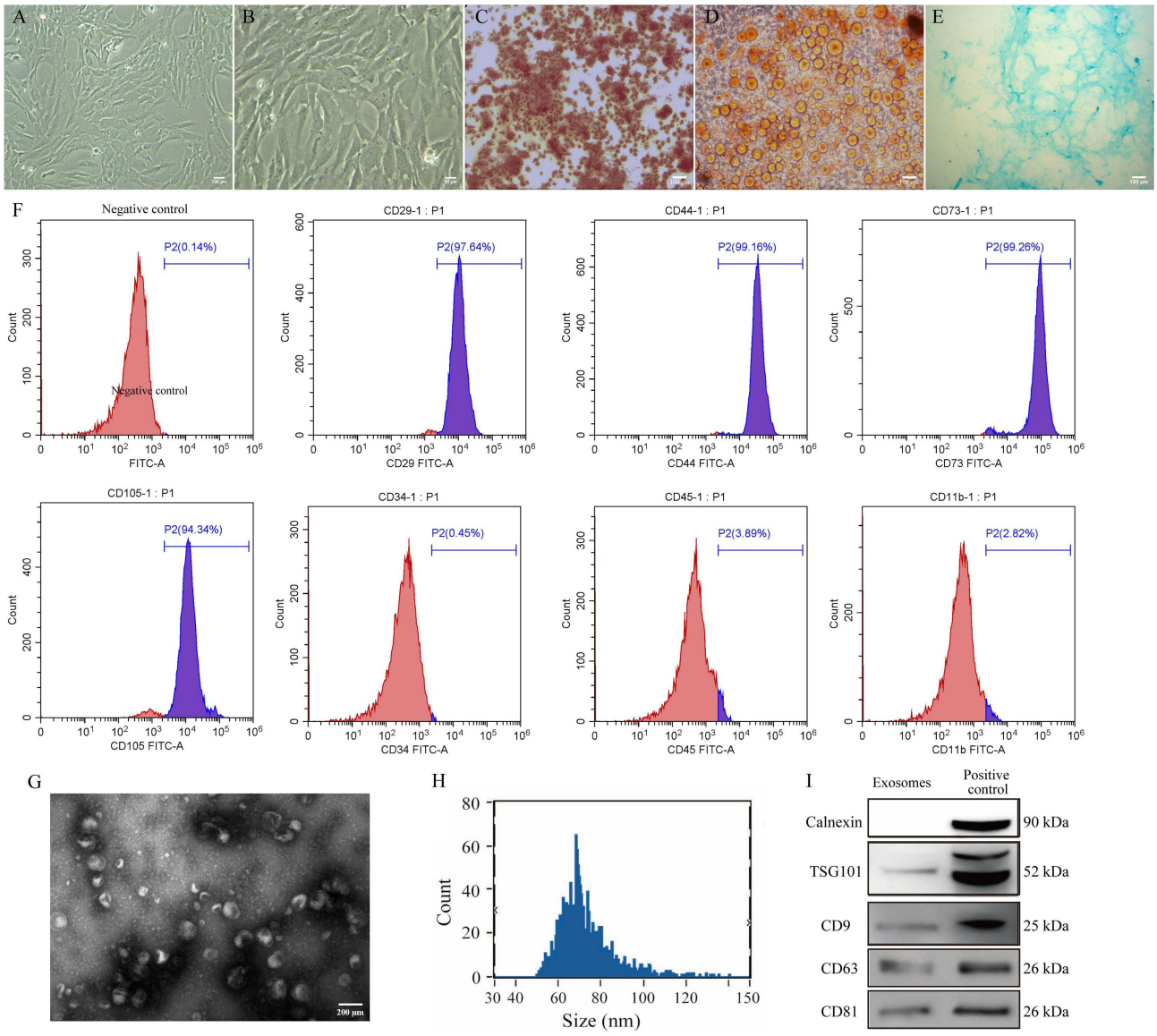

Figure 1 Isolation and identification of BMSCs and exosomes. (**A** and **B**) BMSCs morphology after culturing (scale bar = 100 μm and 50 μm). (**C**) BMSCs were identified based on osteogenic differentiation (scale bar = 100 μm). (**D**) BMSCs were identified based on adipogenic differentiation (scale bar = 100 μm). (**E**) BMSCs were identified based on chondrogenic differentiation (scale bar = 100 μm). (**F**) BMSCs were identified based on flow cytometry analysis for surface marker including CD11b, CD29, CD34, CD44, CD45, CD73, and CD105. (**G**) Exosomes were characterized with transmission electron microscopy. (**H**) The average particle size of exosomes was identified with nanoparticle tracking analysis. (**I**) Exosomes were identified with Western blot.

Abbreviation: BMSCs, Bone marrow mesenchymal stem cells.

https://doi.org/10.2147/IJN.S487097

The exosomes appeared as membrane vesicle structures under a transmission electron microscope (Figure 1G). The average particle size was 72.97 nm (Figure 1H). Western blot showed that the exosomes contained CD9, CD63, CD81, and TSG101, but not calnexin (Figure 1I). These results were consistent with the characteristics of exosomes.

BMSCs-Derived Exosomes Attenuate Apoptosis of CSE-Induced PMVECs

First, we isolated mouse PMVECs via magnetic-activated cell sorting. Figure 2A shows the cobblestone morphology of the cell monolayers (P1) after culturing for 7 days. After subculturing the PMVECs (P2), the morphology was irregular or the spindle type (Figure 2B). Furthermore, immunofluorescence showed that more than 90% of the cells were positive for vWF (red), a typical marker of PMVECs (Figure 2C), thus confirming that we indeed isolated PMVECs.

Then, we treated PMVECs with different concentrations of CSE (0%, 1%, 2.5%, and 4%). The apoptotic rate increased gradually (Figure 2D). Considering that 4% CSE could induce marked cell death, we chose 2.5% CSE for the subsequent experiments. We found treatment of CSE-induced PMVECs with BMSCs-derived exosomes could increase the expression of Bcl-2, and decrease the expression of Bax, and cleaved caspase-3, which indicated a significant anti-apoptotic effect ($p<0.05$) (Figure 2E).

miR-30b is Enriched in BMSCs-Derived Exosomes and Delivered to PMVECs

To identify the miR expression profile and the mechanisms responsible for the protective effect of BMSCs-derived exosomes, we sequenced exosomal miRs. The top ten most abundant miRs were mmu-let-7f-5p, mmu-let-7a-5p, mmu-let-7c-5p, mmu-miR-30b, mmu-let-7d-5p, mmu-miR-34a-5p, mmu-miR-26a-5p, mmu-let-7b-5p, mmu-let-7i-5p, and mmu-miR-143-3p, (Figure 3A and B).

Among the top five miRs in BMSCs-derived exosomes, the expression of miR-30b was the highest, as determined with RT-qPCR (Figure 3C). Furthermore, we found that the expression of miR-30b was significantly decreased in CSE-induced PMVECs. Treatment of CSE-induced PMVECs with BMSCs-derived exosomes increased the expression of miR-30b ($p<0.05$) (Figure 3D). Furthermore, treatment of CSE-induced PMVECs with BMSCs-derived exosomes could reduce the apoptosis, while the knockdown of miR-30b in BMSCs-derived exosomes could increase the apoptosis ($p<0.05$) (Figure 3E), indicating that BMSCs-derived exosomes exert a protective effect on CSE-induced PMVECs perhaps by delivering miR-30b.

miR-30b Attenuates Apoptosis of CSE-Induced PMVECs

The expression of miR-30b decreased gradually as the CSE concentration increased ($p<0.05$) (Figure 4A). Then, we transfected PMVECs with a miR-30b mimic to overexpress miR-30b (Figure 4B). Flow cytometry analysis showed that miR-30b overexpression decreased the apoptotic rate of CSE-induced PMVECs ($p<0.05$) (Figure 4C). Western blot also confirmed that miR-30b overexpression significantly decreased the expression of Bax and cleaved caspase-3, and increased the expression of Bcl-2 ($p<0.05$) (Figure 4D).

miR-30b Attenuates Apoptosis of CSE-Induced PMVECs by Targeting Wnt5a

To investigate the exact effect of miR-30b, we predicted the targets of miR-30b by using two online databases: miRanda and TargetScan. Overlap analysis revealed that Wnt5a is a potential target of miR-30b. Notably, our luciferase reporter assay demonstrated that miR-30b could directly target the 3′-untranslated region (UTR) of Wnt5a (Figure 5A). In addition, the expression of Wnt5a increased gradually as the CSE concentration increased (Figure 5B). Treatment of CSE-induced PMVECs with BMSCs-derived exosomes decreased the expression of Wnt5a, while the expression of Wnt5a was increased after the knockdown of miR-30b in BMSCs-derived exosomes ($p<0.05$) (Figure 5C). In addition, miR-30b overexpression decreased the expression of Wnt5a in CSE-induced PMVECs ($p<0.05$) (Figure 6A). Next, we transfected PMVECs with the pEXP-RB-Mam-EGFP2-Wnt5a plasmid to overexpress Wnt5a. The overexpression of Wnt5a significantly increased PMVECs apoptosis ($p<0.05$) (Figure 6B). Finally, we transfected PMVECs with the miR-30b mimic and the pEXP-RB-Mam-EGFP2-Wnt5a plasmid. As expected, the overexpression of Wnt5a could reverse the anti-apoptotic effect of miR-30b in CSE-induced PMVECs ($p<0.05$) (Figure 6C).

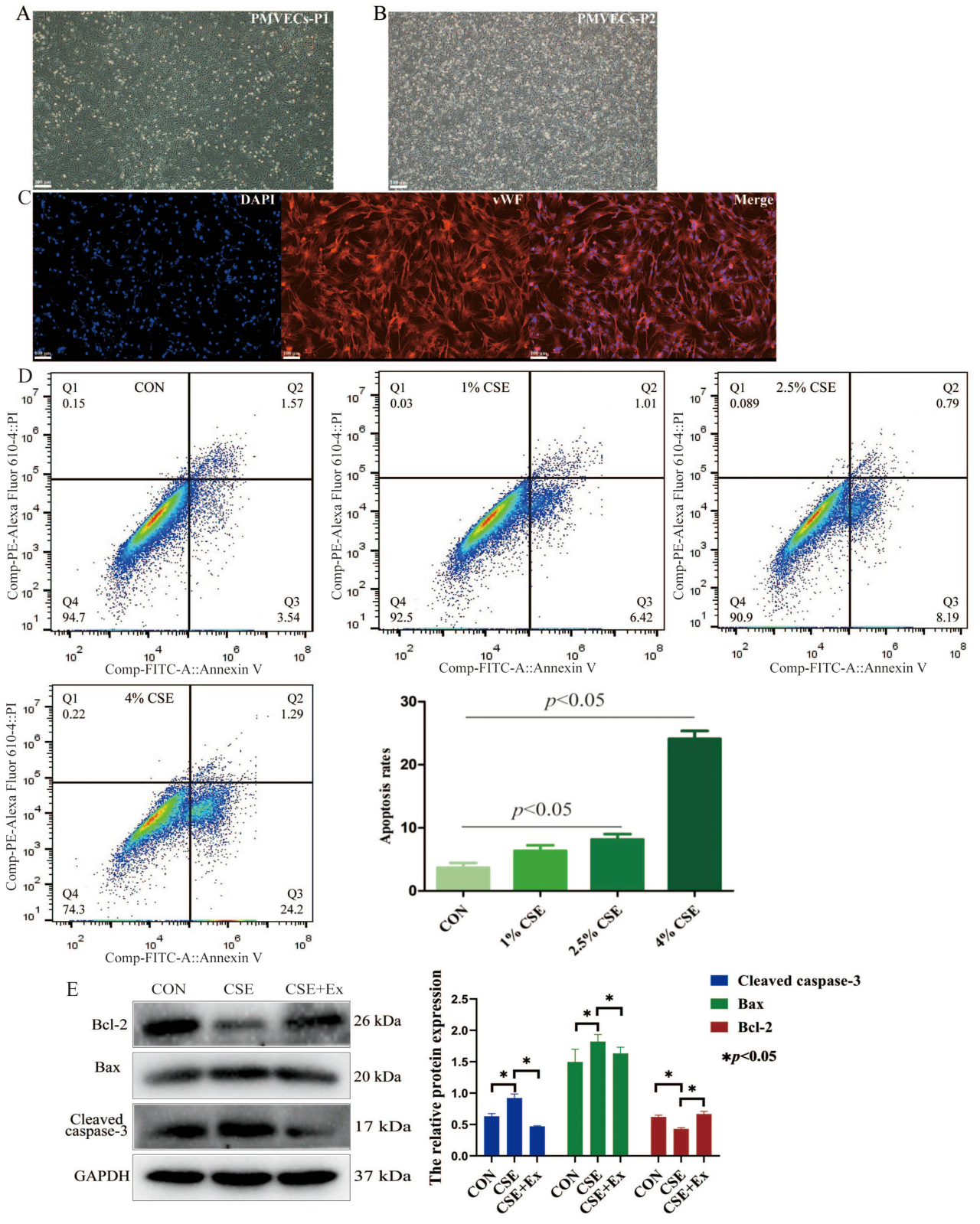

Figure 2 BMSCs-derived exosomes attenuate apoptosis of CSE-induced PMVECs. (**A** and **B**) Normal PMVECs morphology after culturing for P1 and P2 (scale bar = 100 μm); P1, passage 1; P2, passage 2. (**C**) PMVECs were identified based on immunofluorescence staining for vWF (scale bar = 100 μm). (**D**) The apoptosis of CSE-induced PMVECs (CSE delivered at 0%, 1%, 2.5%, and 4%) was detected by flow cytometry analysis. (**E**) The proteins expression of Bax, Bcl-2, and cleaved caspase-3 were detected in CSE-induced PMVECs; CSE, 2.5% CSE.

Abbreviations: CON, Control; Cigarette smoke extract; Ex, Exosomes; PMVECs, Pulmonary microvascular endothelial cells; vWF, von Willebrand factor.

https://doi.org/10.2147/IJN.S487097

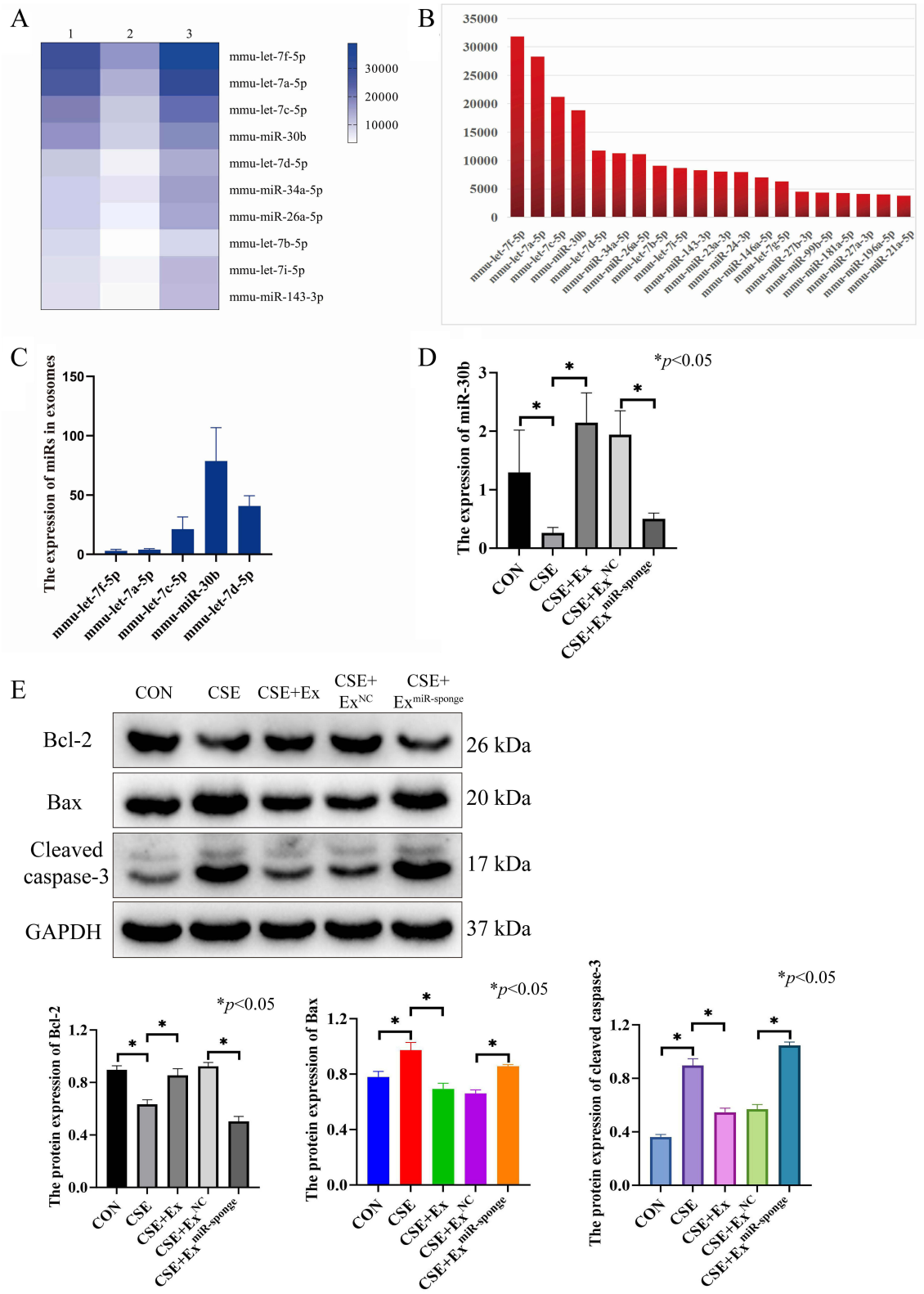

Figure 3 miRs are enriched in BMSCs-derived exosomes and delivered to PMVECs. (**A**) Heatmap of the top ten most abundant miRs in BMSCs-derived exosomes based on miR sequencing. (**B**) Bar chart of the top twenty most abundant miRs in BMSCs-derived exosomes based on miR sequencing (**C**) The expression of top five most abundant miRs in BMSCs-derived exosomes was detected by RT-qPCR. (**D**) The expression of miR-30b in PMVECs was detected by RT-qPCR. (**E**) The proteins expression of Bax, Bcl-2, and cleaved caspase-3 were detected in CSE-induced PMVECs after treatment with BMSCs-derived exosomes. CSE, 2.5% CSE.

Abbreviations: CON, Control; Cigarette smoke extract; Ex, Exosomes; NC, Negative control; PMVECs, Pulmonary microvascular endothelial cells; RT-qPCR: Reverse transcription quantitative polymerase chain reaction; miR-sponge, the knockdown of miR-30b.

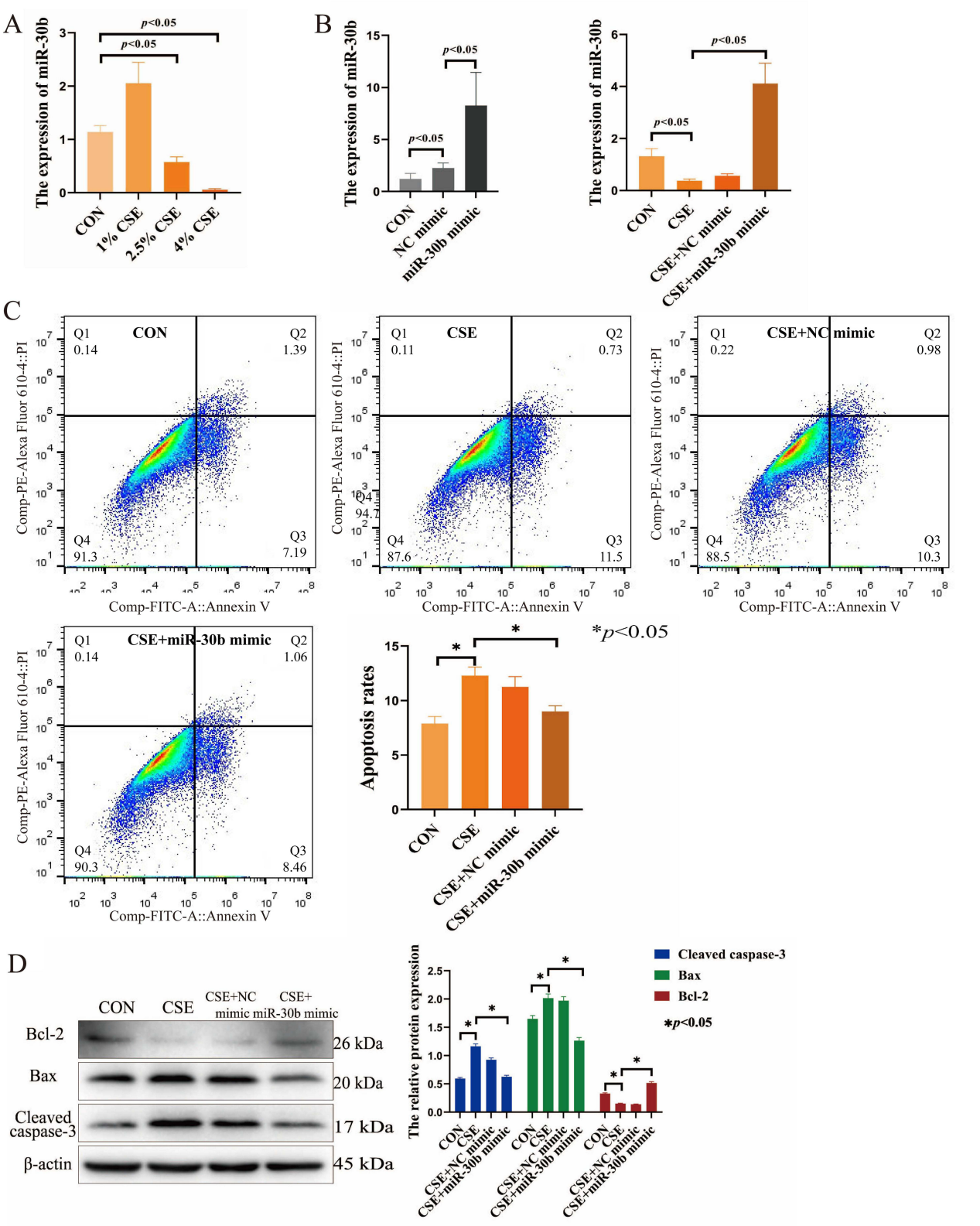

Figure 4 miR-30b attenuates apoptosis of CSE-induced PMVECs. (**A**) The expression of miR-30b in CSE-induced PMVECs was detected by RT-qPCR (CSE delivered at 0%, 1%, 2.5%, and 4%). (**B**) The expression of miR-30b in CSE-induced PMVECs after transfected with miR-30b mimic was detected by RT-qPCR; CSE, 2.5% CSE. (**C**) Apoptosis of CSE-induced PMVECs was detected by flow cytometry analysis; CSE, 2.5% CSE. (**D**) The protein expression of CSE-induced PMVECs was detected by Western blot; CSE, 2.5% CSE. CON, Control; the NC mimic (negative control).

Abbreviations: CSE, Cigarette smoke extract; PMVECs, Pulmonary microvascular endothelial cells.

https://doi.org/10.2147/IJN.S487097

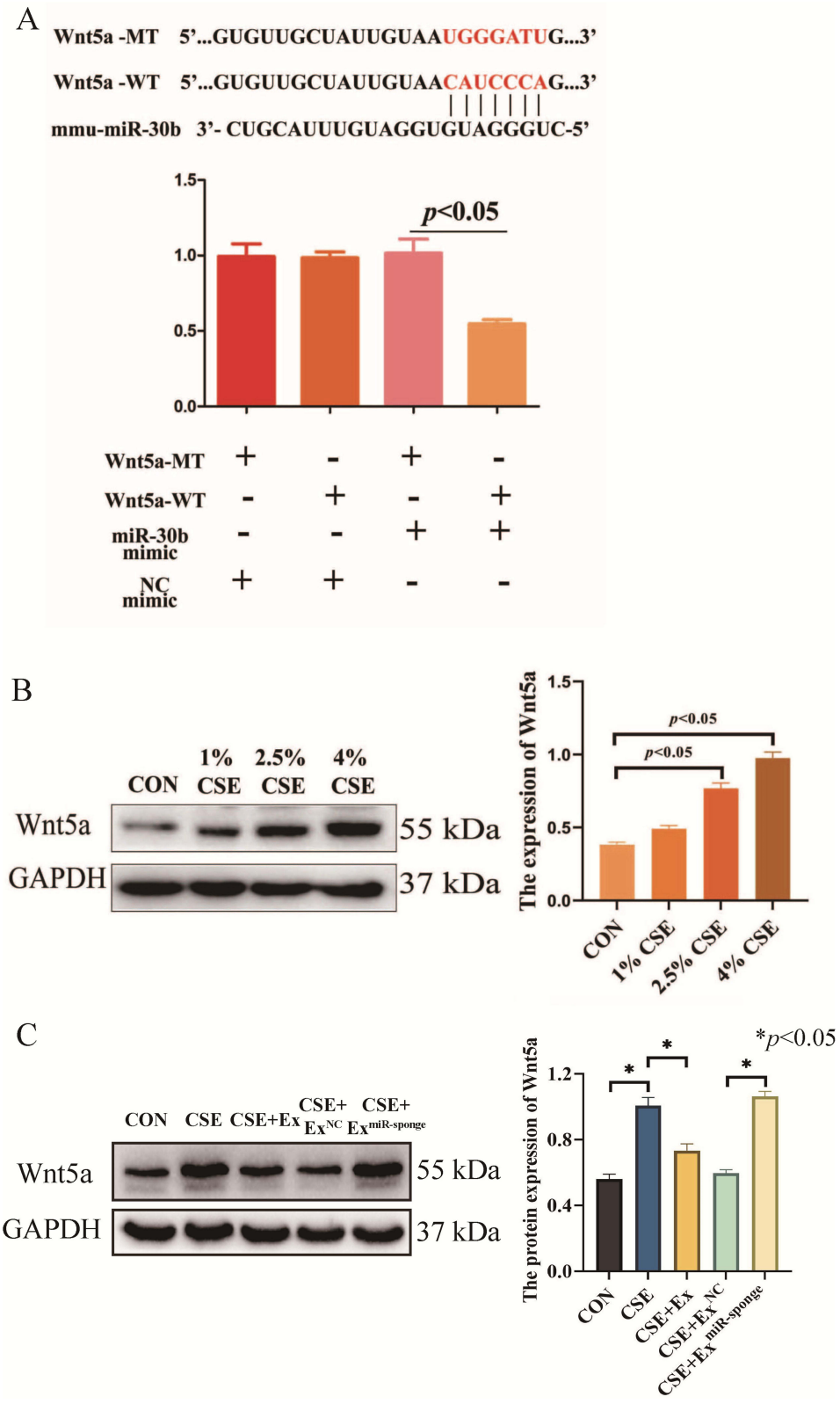

Figure 5 (**A**) A luciferase reporter assay demonstrated that miR-30b could directly target the 3′-UTR of Wnt5a. (**B**) The expression of Wnt5a was detected by Western blot in CSE-induced PMVECs (CSE delivered at 0%, 1%, 2.5%, and 4%). (**C**) The expression of Wnt5a was detected by Western blot in CSE-induced PMVECs after treatment with BMSCs-derived exosomes. CSE, 2.5% CSE. Wnt5a-WT, Wild-type Wnt5a; Wnt5a-MT, Mutant Wnt5a. miR-sponge, the knockdown of miR-30b.

Abbreviations: CON, Control; CSE, Cigarette smoke extract; Ex, Exosomes; NC, Negative control; PMVECs, Pulmonary microvascular endothelial cells; 3′-UTR, 3′-untranslated regions.

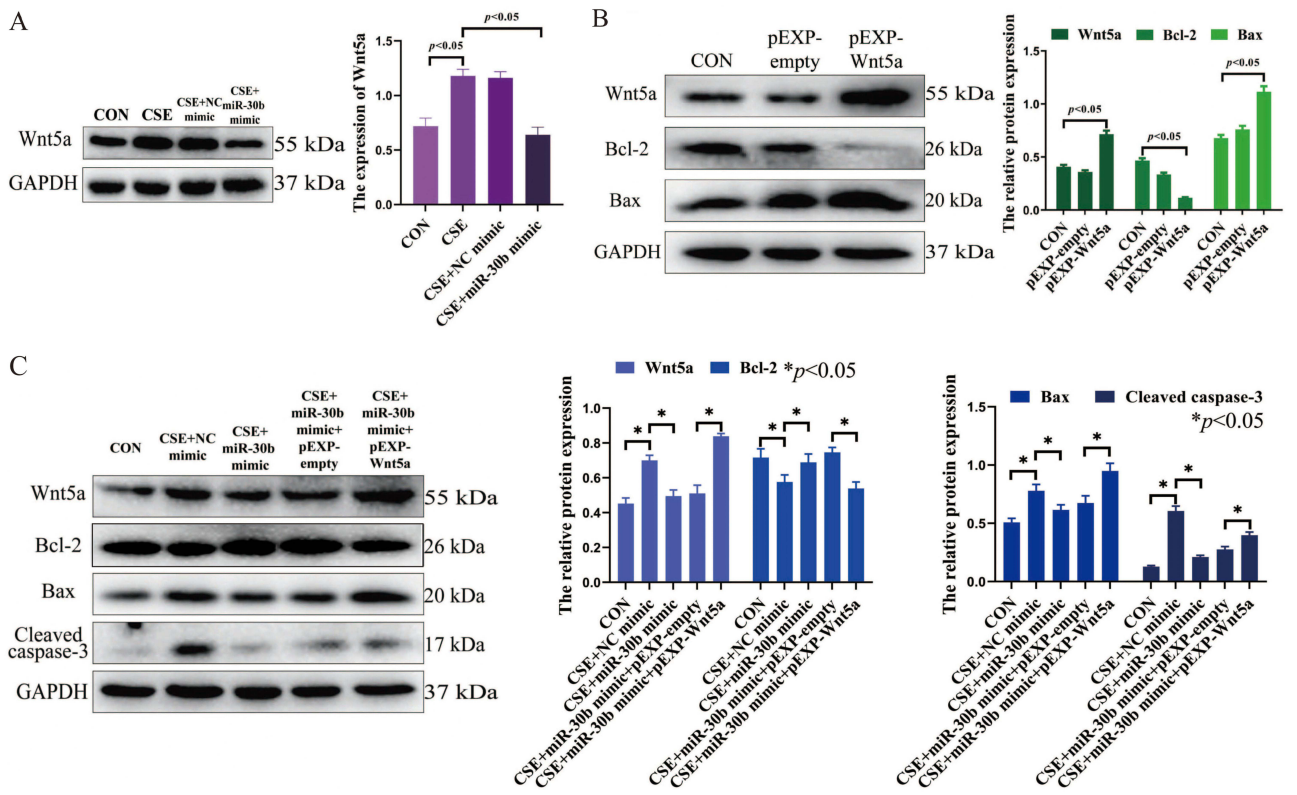

Figure 6 (**A**) miR-30b overexpression decreased the expression of Wnt5a in CSE-induced PMVECs. (**B**) Wnt5a overexpression increased PMVECs apoptosis. (**C**) Wnt5a overexpression reversed the anti-apoptotic effect of miR-30b in CSE-induced PMVECs; CSE, 2.5% CSE.
Abbreviations: CON, Control; CSE, Cigarette smoke extract; PMVECs, Pulmonary microvascular endothelial cells.

The Effects of BMSCs-Derived Exosomes in the Lung Tissue of COPD Mice

To identify the effects of BMSCs-derived exosomes and miR-30b in COPD mice, we administered an intratracheal instillation of BMSCs-derived exosomes and HBLV-mmu-miR-30b (miR-30b overexpression) to mice. Figure 7A shows a schematic outline of the animal experiment. The lung tissue of COPD mice showed enlarged alveolar spaces, thinner alveolar septa, and destruction of alveolar walls relative to control mice. In addition, COPD mice showed a higher DI and MLI ($p<0.05$). After treating COPD mice with BMSCs-derived exosomes and HBLV-mmu-miR-30b, the above changes were significantly improved ($p<0.05$) (Figure 7B). In addition, the expression of miR-30b was significantly decreased in COPD mice, while treatment with BMSCs-derived exosomes and HBLV-mmu-miR-30b significantly increased the expression of miR-30b in the lung tissues ($p<0.05$) (Figure 7C). TUNEL and CD31 double staining showed that COPD mice had more apoptotic PMVECs compared with control mice ($p<0.05$). However, the above change was reversed after treatment with BMSCs-derived exosomes and HBLV-mmu-miR-30b ($p<0.05$) (Figure 8). Furthermore, COPD mice showed a considerable increase in the expression of Bax, and cleaved caspase-3, but a decrease in the expression of Bcl-2. After treatment with BMSCs-derived exosomes and HBLV-mmu-miR-30b, the above protein expression changes were reversed ($p<0.05$) (Figure 9A). Moreover, miR-30b overexpression and treatment with BMSCs-derived exosomes showed the same protective effect in COPD mice.

In addition, the expression of Wnt5a was increased in COPD mice compared with the control mice ($p<0.05$), while the expression of Wnt5a was decreased after treatment with BMSCs-derived exosomes and HBLV-mmu-miR-30b compared with COPD mice ($p<0.05$) (Figure 9A and B).

https://doi.org/10.2147/IJN.S487097

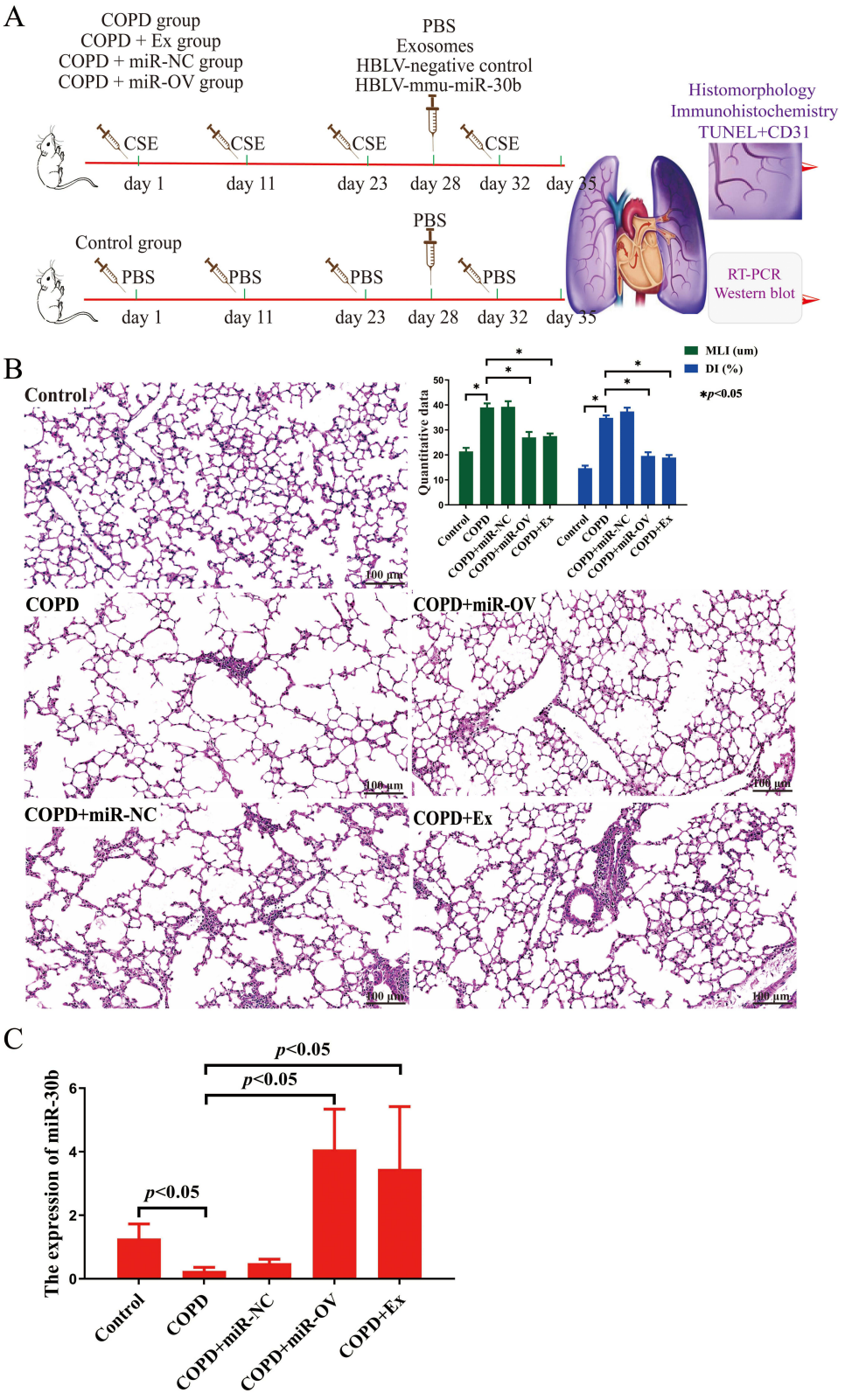

Figure 7 The effects of BMSCs-derived exosomes in the lung tissue of COPD mice. (**A**) Schematic outline of the animal experiment. (**B**) HE staining of mice lung tissue (scale bar = 100 μm). (**C**) The expression of miR-30b in mice lung tissues was detected by RT-qPCR. N=8 mice per group; CSE, Cigarette smoke extract; COPD, Chronic obstructive pulmonary disease; DI, Destructive index; MLI, Mean linear intercept; RT-qPCR: Reverse transcription quantitative polymerase chain reaction. The COPD + Ex group was given an BMSCs exosomes; the COPD + miR-NC group was given an HBLV-ZsGreen-PURO negative control; the COPD + miR-OV group was given an HBLV-mmu-miR-30b–ZsGreen-PURO to achieve miR-30b overexpression.

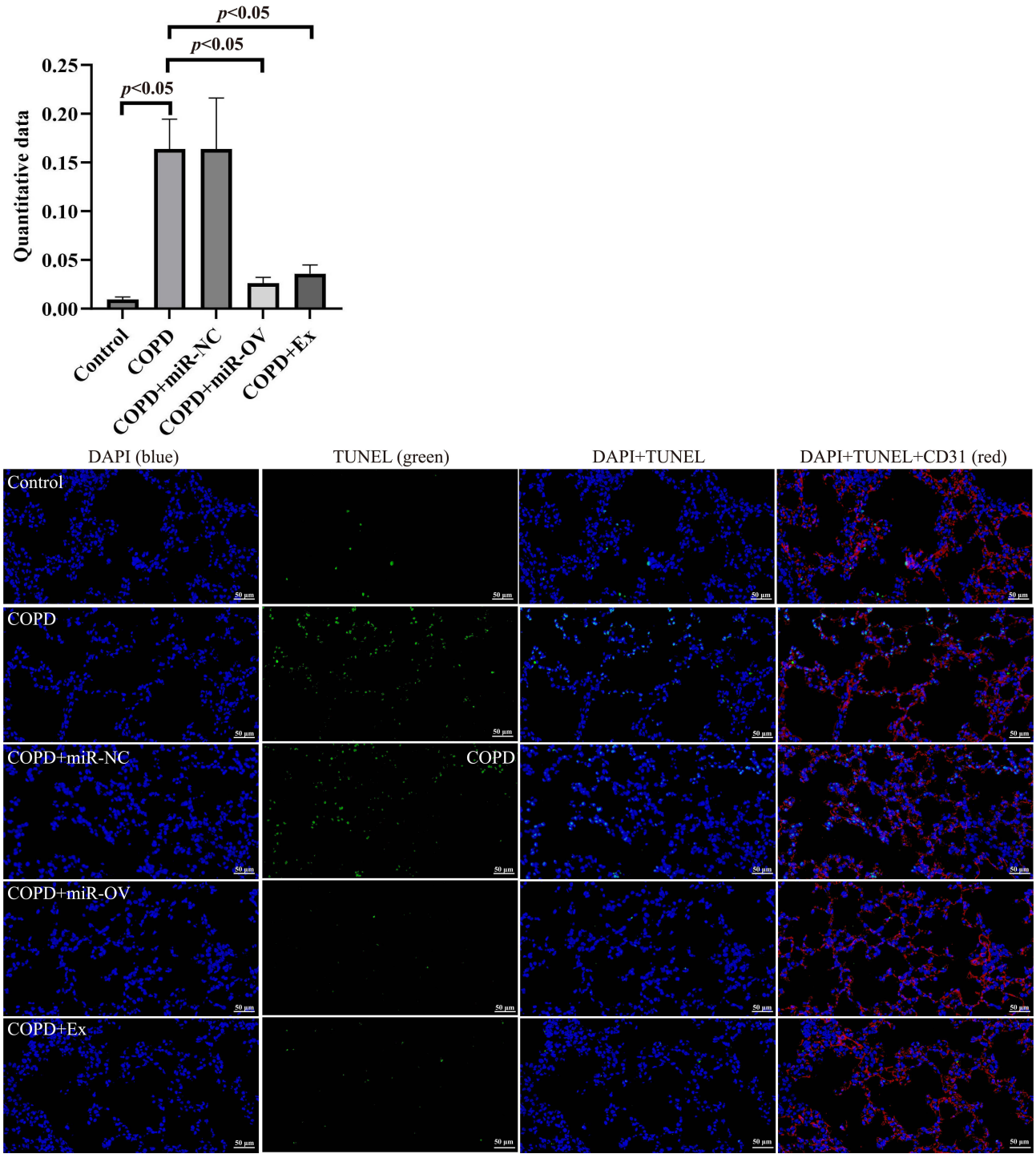

Figure 8 The effects of BMSCs-derived exosomes in the lung tissue of COPD mice. TUNEL and CD31 double staining was used to detect apoptosis in mice lung tissue. The colors indicate all cells (blue), apoptotic cells (green) and PMVECs (red) (scale bar = 50 μm). N=8 mice per group; COPD, Chronic obstructive pulmonary disease; TUNEL, Terminal deoxynucleotidyl transferase-mediated dUTP nick end labelling. The COPD + Ex group was given an BMSCs exosomes; the COPD + miR-NC group was given an HBLV-ZsGreen-PURO negative control; the COPD + miR-OV group was given an HBLV-mmu-miR-30b–ZsGreen-PURO to achieve miR-30b overexpression.

The Expression of miR-30b and Wnt5a in Patients with COPD

To evaluate the effect of miR-30b and Wnt5a in humans, we collected lung tissue samples from control participants and patients with COPD. The clinical characteristics of the participants are shown in Supplement Table 1. There were no significant differences in sex, age, and body mass index. Compared with the control participants, miR-30b expression

https://doi.org/10.2147/IJN.S487097

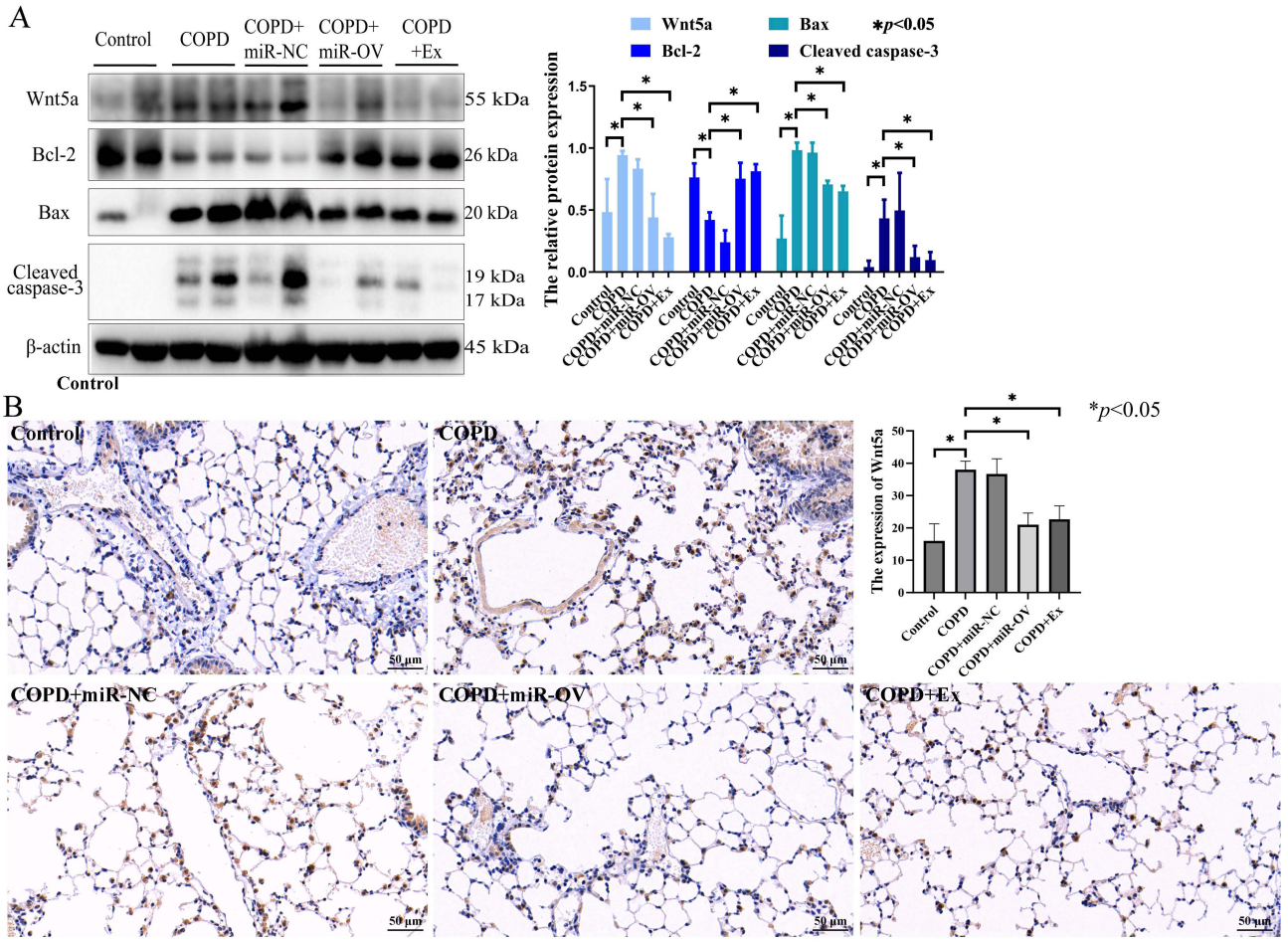

Figure 9 The effects of BMSCs-derived exosomes in the lung tissue of COPD mice. (**A**) The proteins expression of Bax, Bcl-2, cleaved caspase-3, and Wnt5a were detected by Western blot in mice lung tissue. (**B**) The Wnt5a expression was detected by immunohistochemistry in mice lung tissue (scale bar = 50 μm). N=8 mice per group; COPD, Chronic obstructive pulmonary disease; The COPD + Ex group was given an BMSCs exosomes; the COPD + miR-NC group was given an HBLV-ZsGreen-PURO negative control; the COPD + miR-OV group was given an HBLV-mmu-miR-30b–ZsGreen-PURO to achieve miR-30b overexpression.

was significantly decreased in patients with COPD ($p<0.05$) (Figure 10A). In addition, compared with the control participants, Wnt5a expression was significantly increased in patients with COPD ($p<0.05$) (Figure 10B and C).

Discussion

Previous studies have shown that the PMVECs apoptosis is involved in the development of COPD. The apoptotic rate of pulmonary vascular endothelial cells is significantly correlated with the degree of lung function impairment and emphysema. Therefore, in this study, we selected marginal lung tissues (within 3 mm) to isolate normal PMVECs. After enzymatic dispersion of lung tissues into a cellular suspension, we selected CD31-positive cells by using magnetic-activated cell sorting and cultured the cells in endothelial-specific growth conditions.[22] Immunofluorescence staining confirmed that more than 90% of the cells were positive for vWF, which is the specific surface marker of endothelial cells. Hence, our isolated PMVECs were highly pure.

BMSCs are currently the most commonly used stem cells. Extraction of mesenchymal stem cells with high purity is crucial. The available methods for extracting mesenchymal stem cells include the whole bone marrow adherence method and density gradient centrifugation. The minimum standards for mesenchymal stem cells identification include: the ability to adhere to the wall of a culture dish; express CD105, CD73, and CD90, but not CD34 and CD45 on the surface; and the ability to differentiate into osteocytes and adipocytes.[23] In addition, Ragni et al[24] found that BMSCs are negative for CD34 and CD45, while strongly positive for CD44. In addition, Song et al[25] found that BMSCs expressed CD 29 and

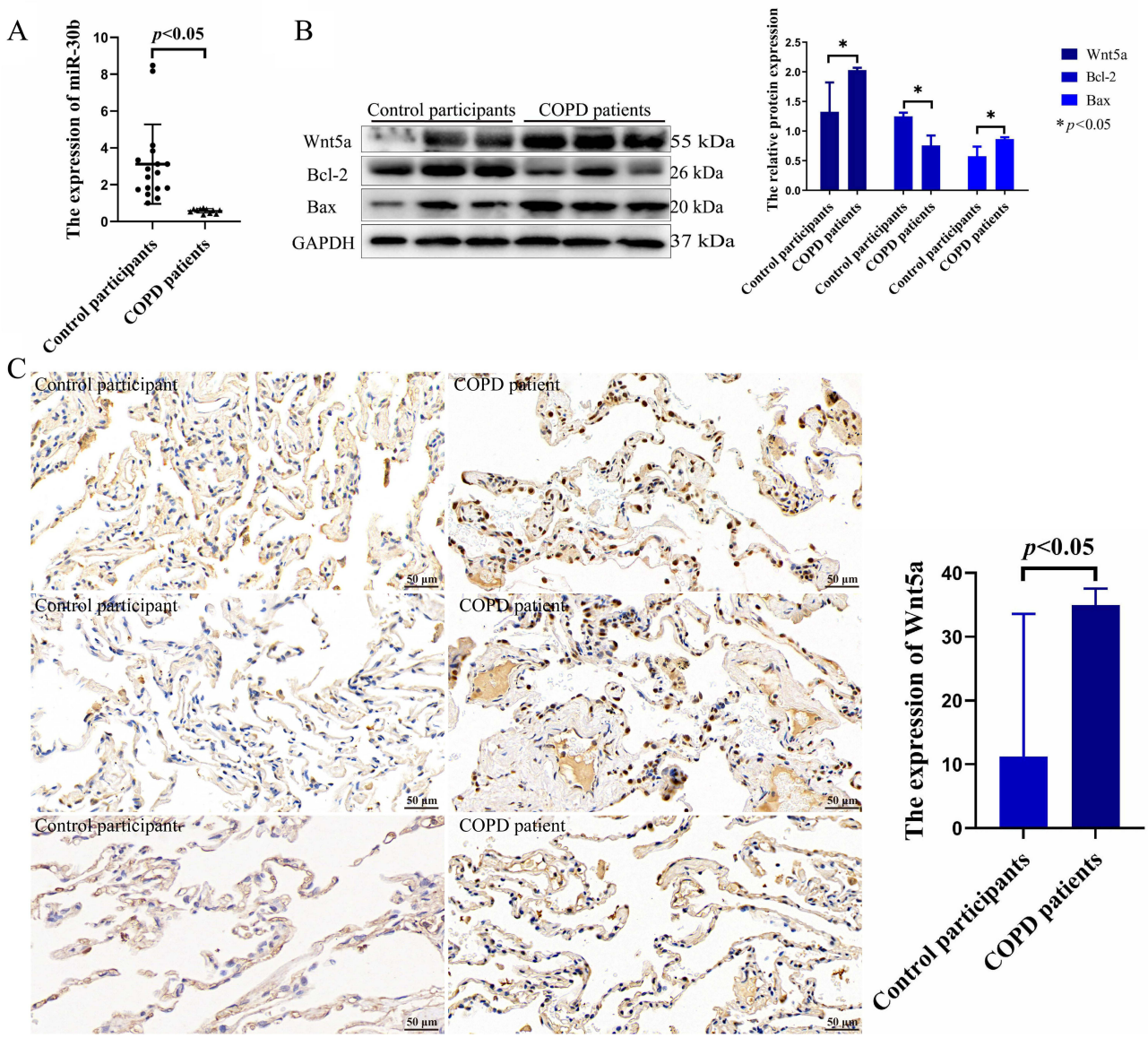

Figure 10 The expression of miR-30b and Wnt5a in patients with COPD. (**A**) The expression of miR-30b was detected in control participants and COPD patients. (**B**) The expression of Wnt5a, Bcl-2, and Bax were detected by Western blot in control participants and COPD patients. (**C**) The expression of Wnt5a was detected by immunohistochemistry in lung tissue (scale bar = 50 μm). Control participants (N=17) and COPD patients (N=11).
Abbreviation: COPD, Chronic obstructive pulmonary disease.

CD90, but not CD45. In our study, we extracted BMSCs that expressed CD29, CD44, CD73, and CD105, but not CD34, CD45, and CD11b. In addition, the BMSCs could differentiate into osteocytes, adipocytes, and chondrocytes. This confirmed that the cells we extracted from bone marrow are consistent with mesenchymal stem cells characteristics.

Exosomes can deliver miRs and proteins to recipient cells, and also participate in intercellular communication. Mesenchymal stem cells-derived exosomes are rich in a variety of active substances, and have shown powerful therapeutic effects on cells injury and several diseases.[26,27] In the present study, we found that BMSCs-derived exosomes could reduce apoptosis of CSE-induced PMVECs. Furthermore, to explore the underlying mechanisms by which BMSCs-derived exosomes relieve cells injury, we identified the miR expression profile in BMSCs-derived exosomes: let-7-5p, miR-30b, miR-34a-5p, miR-26a-5p, and miR-23a-3p were enriched. This is different from the results reported by Chen et al[26] and Cao et al,[27] perhaps because we extracted exosomes from mouse BMSCs, while they extracted exosomes from human BMSCs. Furthermore, based on RT-qPCR, we found that miR-30b expression was the highest in BMSC-derived exosomes. Treatment with BMSCs-derived exosomes could increase the expression of miR-30b in CSE-

https://doi.org/10.2147/IJN.S487097

induced PMVECs. Notably, Gong et al[28] found that miR-30b could be delivered to endothelial cells when mesenchymal stem cells-derived exosomes were co-cultured with umbilical vein endothelial cells, a finding similar to our results. In addition, treatment of CSE-induced PMVECs with BMSCs-derived exosomes could reduce the apoptosis, while the knockdown of miR-30b in BMSCs-derived exosomes could increase the apoptosis. Furthermore, we found that the overexpression of miR-30b could inhibit the apoptosis of CSE-induced PMVECs. This implies that BMSCs-derived exosomes may exert a protective effect by delivering miR-30b to CSE-induced PMVECs. In fact, Chen et al[26] found that mesenchymal stem cells-derived exosomes could reduce apoptosis in hypoxia-induced beta cells by delivering miR-21. Jahangiri et al[29] found that mesenchymal stem cells-derived exosomes could suppress proliferation, migration, invasion, and metastasis while inducing the apoptosis of the colorectal cancer cells via miR-100. However, the detail mechanism needs to be further explored.

Wnt5a is a secreted glycoprotein that belongs to the noncanonical Wnt family. Wnt5a and it's signaling pathway exhibit dual effects on angiogenesis and may be a potential target for the treatment of angiogenesis-related diseases.[30] On the one hand, Wnt5a can promote angiogenesis.[31] However, in some reports, Wnt5a may suppress angiogenesis, reducing both endothelial cell proliferation and capillary length.[32] In the present study, the expression of Wnt5a was significantly increased in CSE-induced PMVECs, and the overexpression of Wnt5a significantly increased the apoptosis of PMVECs. In fact, Wang et al[33] found that the fine-particulate matter ($PM_{2.5}$) aggravates CSE-induced airway inflammation via Wnt5a-extracellular signal-regulated kinase pathway in COPD. $PM_{2.5}$ induces lung inflammation and fibrosis via airway smooth muscle cell expression of the Wnt5a/JNK pathway.[34] Furthermore, we found that miR-30b could reduce CSE-induced PMVECs apoptosis by targeting Wnt5a. A previous study confirmed that miR-30b could inhibit osteoblast differentiation through targeting BCL6.[35] Upregulated miR-374a-5p drives psoriasis pathogenesis through WIF1 down-regulation and Wnt5a/NF-κB activation.[36] miR-141-3p reduces cell migration and proliferation in an in vitro model of atherosclerosis by targeting Wnt5a.[37] These findings are similar to our results.

Furthermore, to explore the role of BMSCs-derived exosomes in lung tissue of COPD mice, we used an intraperitoneal injection of CSE to establish a COPD mouse model. We previously confirmed that intraperitoneal injection of mice with CSE could successfully construct a COPD mouse model and that PMVECs apoptosis is increased in these mice, a change that is significantly correlated with the impaired lung function and emphysema. In addition, previous studies have shown that COPD established by intraperitoneal injection of CSE has a similar phenotype with what is induced by exposure to cigarette smoke.[5–7,18] In addition, we treated the mice with BMSCs-derived exosomes and HBLV-mmu-miR-30b via intratracheal instillation. Compared with intravenous administration, intratracheal instillation allows full distribution of the drug directly to the lung tissues. Several studies have confirmed that the safety and efficacy of intratracheal instillation.[38–40] We found that the expression of miR-30b was significantly decreased in COPD mouse lung tissue. Consistently, Fu et al[41] found that the miR-30b was downregulated in the lung of COPD rats. Izzotti et al[42] also found that the expression of miR-30b was significantly decreased in cigarette smoke-induced rats. These findings indicate the potential role of miR-30b in COPD progression. Furthermore, we found that BMSCs-derived exosomes could improve the damage of CSE-induced COPD, ameliorate PMVECs apoptosis, and decrease the expression of Wnt5a, and increase the expression of miR-30 in lung tissue. What's more, we conducted a direct comparison between the overexpression of miR-30b and BMSCs-derived exosomes, and there was a same protective effect between the overexpression of miR-30b and BMSCs-derived exosomes in COPD mice. This implies that BMSCs-derived exosomes might exert a protective effect perhaps by delivering miR-30b in COPD mice. Wu et al[43] found that exosomal miR-30b-5p derived from BMSCs could promote non-small cell lung cancer cell apoptosis and prevent tumorigenesis in nude mice via the EZH2/PI3K/AKT axis. Zhao et al[44] showed that mesenchymal stem cells-derived exosomes reduced myocardial ischemia/reperfusion injury in mice by shuttling miR-182. In addition, mesenchymal stem cells-derived exosomes inhibited vascular remodeling and hypoxic pulmonary hypertension in hypoxic mice and increased the expression of miR-204.[45]

We also determined the expression of miR-30b and Wnt5a in the lung tissue of patients with COPD. We found that the miR-30b was decreased, while Wnt5a was increased in COPD patients. Baarsma et al[14] found that Wnt5a was increased in primary lung fibroblasts from patients with COPD and induced by COPD-related stimuli, such as cigarette smoke.

Our study has limitations. We directly treated PMVECs with miR-30b to confirm its impact on apoptosis, and then found that BMSCs-derived exosomes inhibit PMVECs apoptosis perhaps by delivering miR-30b, a finding similar to a previous study.[46] Furthermore, a better confirmation of the protective effect of BMSCs-derived exosomes would have been to pretreat BMSCs with miR-30b, and to treat PMVECs with these exosomes. We will use this approach in our future research. In addition, we examined a relatively small number of patients with COPD, although we included as many cases as possible.

Conclusions

BMSCs-derived exosomes could improve the damage of COPD perhaps by delivering miR-30b. miR-30b could reduce apoptosis of CSE-induced PMVECs by targeting Wnt5a.

Abbreviations

BMSCs, Bone marrow mesenchymal stem cells; COPD, Chronic obstructive pulmonary disease; CSE, Cigarette smoke extract; DI, Destructive index; DAPI, 4′,6-diamidino-2′-phenylindole; Ex, Exosomes; miR, miRNA; HE staining, Hematoxylin-eosin staining; MLI, Mean linear intercept; PMVECs, Pulmonary microvascular endothelial cells; PBS, Phosphate buffered saline; RT-qPCR, Reverse transcription quantitative polymerase chain reaction; TUNEL, Terminal deoxynucleotidyl transferase-mediated dUTP nick end labeling; 3′-UTR, 3′-untranslated regions; vWF, Von Willebrand factor.

Data Sharing Statement

The datasets used and analyzed during the current study are available from the corresponding author on reasonable request.

Ethics Approval and Consent to Participate

This study was approved by the Ethics Committee of the Second Xiangya Hospital of Central South University (Number: 2022200 and Z0208-01) (Hunan, China) and conformed to the guidelines principles for research involving animals and human beings.

Author Contributions

All authors made a significant contribution to the work reported, whether that is in the conception, study design, execution, acquisition of data, analysis and interpretation, or in all these areas; took part in drafting, revising or critically reviewing the article; gave final approval of the version to be published; have agreed on the journal to which the article has been submitted; and agree to be accountable for all aspects of the work.

Funding

This work was supported by National Natural Science Foundation of China (Grant numbers: 81970044 and 82270045 to Ping Chen).

Disclosure

The authors declare that they have no competing interests.

References

1. Soriano JB, Kendrick PJ, Paulson KR, GBD Chronic Respiratory Disease Collaborators. Prevalence and attributable health burden of chronic respiratory diseases, 1990-2017: a systematic analysis for the global burden of disease study 2017. *Lancet Respir Med*. 2020;8(6):585–596. doi:10.1016/S2213-2600(20)30105-3
2. Lareau SC, Fahy B, Meek P, Wang A. Chronic obstructive pulmonary disease (COPD). *Am J Respir Crit Care Med*. 2019;199(1):1–P2. doi:10.1164/rccm.1991P1
3. GOLD Executive Committee. Global strategy for the diagnosis, management and prevention of chronic obstructive pulmonary disease (2017 REPORT). Availale from: https://goldcopd.org/. Accessed November, 2017.

4. Song Q, Chen P, Liu XM. The role of cigarette smoke-induced pulmonary vascular endothelial cell apoptosis in COPD. *Respir Res*. 2021;22(1):39. doi:10.1186/s12931-021-01630-1
5. He ZH, Chen P, Chen Y, et al. Comparison between cigarette smoke-induced emphysema and cigarette smoke extract-induced emphysema. *Tob Induc Dis*. 2015;13(1):6. doi:10.1186/s12971-015-0033-z
6. Zeng H, Shi Z, Kong X, et al. Involvement of B-cell CLL/lymphoma 2 promoter methylation in cigarette smoke extract-induced emphysema. *Exp Biol Med*. 2016;241(8):808–816. doi:10.1177/1535370216635759
7. Chen Y, Hanaoka M, Droma Y, Chen P, Voelkel NF, Kubo K. Endothelin-1 receptor antagonists prevent the development of pulmonary emphysema in rats. *Eur Respir J*. 2010;35(4):904–912. doi:10.1183/09031936.00003909
8. Chen X, Wang F, Huang Z, Wu Y, Geng J, Wang Y. Clinical applications of mesenchymal stromal cell-based therapies for pulmonary diseases: an update and concise review. *Int J Med Sci*. 2021;18(13):2849–2870. doi:10.7150/ijms.59218
9. Kalluri R, LeBleu VS. The biology, function, and biomedical applications of exosomes. *Science*. 2020;367(6478):eaau6977. doi:10.1126/science.aau6977
10. Li Y, Yin Z, Fan J, Zhang S, Yang W. The roles of exosomal miRNAs and lncRNAs in lung diseases. *Signal Transduct Target Ther*. 2019;4:47. doi:10.1038/s41392-019-0080-7
11. Shang R, Lee S, Senavirathne G, Lai EC. microRNAs in action: biogenesis, function and regulation. *Nat Rev Genet*. 2023;24(12):816–833. doi:10.1038/s41576-023-00611-y
12. Boateng E, Krauss-Etschmann S. miRNAs in lung development and diseases. *Int J Mol Sci*. 2020;21(8):2765. doi:10.3390/ijms21082765
13. Park S, Kim M, Park M, Jin Y, Lee SJ, Lee H. Specific upregulation of extracellular miR-6238 in particulate matter-induced acute lung injury and its immunomodulation. *J Hazard Mater*. 2023;445:130466. doi:10.1016/j.jhazmat.2022.130466
14. Baarsma HA, Skronska-Wasek W, Mutze K, et al. Noncanonical WNT-5A signaling impairs endogenous lung repair in COPD. *J Exp Med*. 2017;214(1):143–163. doi:10.1084/jem.20160675
15. Kim KB, Kim DW, Kim Y, et al. WNT5A-RHOA signaling is a driver of tumorigenesis and represents a therapeutically actionable vulnerability in small cell lung cancer. *Cancer Res*. 2022;82(22):4219–4233. doi:10.1158/0008-5472.CAN-22-1170
16. Soleimani M, Nadri S. A protocol for isolation and culture of mesenchymal stem cells from mouse bone marrow. *Nat Protoc*. 2009;4(1):102–106. doi:10.1038/nprot.2008.221
17. Zhang J, Guan J, Niu X, et al. Exosomes released from human induced pluripotent stem cells-derived MSCs facilitate cutaneous wound healing by promoting collagen synthesis and angiogenesis. *J Transl Med*. 2015;13:49. doi:10.1186/s12967-015-0417-0
18. Chen Y, Hanaoka M, Chen P, Droma Y, Voelkel NF, Kubo K. Protective effect of beraprost sodium, a stable prostacyclin analog, in the development of cigarette smoke extract-induced emphysema. *Am J Physiol Lung Cell Mol Physiol*. 2009;296(4):L648–56. doi:10.1152/ajplung.90270.2008
19. Genschmer KR, Russell DW, Lal C, et al. Activated PMN exosomes: pathogenic entities causing matrix destruction and disease in the lung. *Cell*. 2019;176(1–2):113–126.e15. doi:10.1016/j.cell.2018.12.002
20. Song Q, Zhou ZJ, Cai S, Chen Y, Chen P. Oxidative stress links the tumour suppressor p53 with cell apoptosis induced by cigarette smoke. *Int J Environ Health Res*. 2022;32(8):1745–1755. doi:10.1080/09603123.2021.1910211
21. Liu X, Ma Y, Luo L, et al. Dihydroquercetin suppresses cigarette smoke induced ferroptosis in the pathogenesis of chronic obstructive pulmonary disease by activating Nrf2-mediated pathway. *Phytomedicine*. 2022;96:153894. doi:10.1016/j.phymed.2021.153894
22. Alphonse RS, Vadivel A, Zhong S, et al. The isolation and culture of endothelial colony-forming cells from human and rat lungs. *Nat Protoc*. 2015;10(11):1697–1708. doi:10.1038/nprot.2015.107
23. Dominici M, Le Blanc K, Mueller I, et al. Minimal criteria for defining multipotent mesenchymal stromal cells. The international society for cellular therapy position statement. *Cytotherapy*. 2006;8(4):315–317. doi:10.1080/14653240600855905
24. Ragni E, Montemurro T, Montelatici E, et al. Differential microRNA signature of human mesenchymal stem cells from different sources reveals an ”environmental-niche memory” for bone marrow stem cells. *Exp Cell Res*. 2013;319(10):1562–1574. doi:10.1016/j.yexcr.2013.04.002
25. Song K, Huang M, Shi Q, Du T, Cao Y. Cultivation and identification of rat bone marrow-derived mesenchymal stem cells. *Mol Med Rep*. 2014;10(2):755–760. doi:10.3892/mmr.2014.2264
26. Chen J, Chen J, Cheng Y, et al. Mesenchymal stem cell-derived exosomes protect beta cells against hypoxia-induced apoptosis via miR-21 by alleviating ER stress and inhibiting p38 MAPK phosphorylation. *Stem Cell Res Ther*. 2020;11(1):97. doi:10.1186/s13287-020-01610-0
27. Cao JY, Wang B, Tang TT, et al. Exosomal miR-125b-5p deriving from mesenchymal stem cells promotes tubular repair by suppression of p53 in ischemic acute kidney injury. *Theranostics*. 2021;11(11):5248–5266. doi:10.7150/thno.54550
28. Gong M, Yu B, Wang J, et al. Mesenchymal stem cells release exosomes that transfer miRNAs to endothelial cells and promote angiogenesis. *Oncotarget*. 2017;8(28):45200–45212. doi:10.18632/oncotarget.16778
29. Jahangiri B, Khalaj-Kondori M, Asadollahi E, Purrafee Dizaj L, Sadeghizadeh M. MSC-derived exosomes suppress colorectal cancer cell proliferation and metastasis via miR-100/mTOR/miR-143 pathway. *Int J Pharm*. 2022;627:122214. doi:10.1016/j.ijpharm.2022.122214
30. Shi YN, Zhu N, Liu C, et al. Wnt5a and its signaling pathway in angiogenesis. *Clin Chim Acta*. 2017;471:263–269. doi:10.1016/j.cca.2017.06.017
31. Wan X, Guan S, Hou Y, et al. FOSL2 promotes VEGF-independent angiogenesis by transcriptionnally activating Wnt5a in breast cancer-associated fibroblasts. *Theranostics*. 2021;11(10):4975–4991. doi:10.7150/thno.55074
32. Goodwin AM, Kitajewski J, D’Amore PA. Wnt1 and Wnt5a affect endothelial proliferation and capillary length; Wnt2 does not. *Growth Factors*. 2007;25(1):25–32. doi:10.1080/08977190701272933
33. Wang Z, Zhao J, Wang T, Du X, Xie J. Fine-particulate matter aggravates cigarette smoke extract-induced airway inflammation via Wnt5a-ERK pathway in COPD. *Int J Chron Obstruct Pulmon Dis*. 2019;14:979–994. doi:10.2147/COPD.S195794
34. Zou W, Liu S, Ye D, et al. PM2.5 induces lung inflammation and fibrosis via airway smooth muscle cell expression of the Wnt5a/JNK pathway. *J Thorac Dis*. 2023;15(11):6094–6105. doi:10.21037/jtd-23-780
35. Luo Y, Zhou F, Wu X, Li Y, Ye B. miR-30b-5p inhibits osteoblast differentiation through targeting BCL6. *Cell Cycle*. 2022;21(6):630–640. doi:10.1080/15384101.2022.2031428
36. Ma J, Gan L, Chen H, et al. Upregulated miR-374a-5p drives psoriasis pathogenesis through WIF1 downregulation and Wnt5a/NF-κB activation. *Cell Signal*. 2024;119:111171. doi:10.1016/j.cellsig.2024.111171
37. Zhang F, Sun P, Yuan N. miR-141-3p reduces cell migration and proliferation in an in vitro modelof atherosclerosis by targeting Wnt5a. *J Invest Surg*. 2022;35(3):598–604. doi:10.1080/08941939.2021.1904467

38. Guillamat-Prats R, Puig. F, Camprubí-Rimblas M, et al. Intratracheal instillation of alveolar type II cells enhances recovery from acute lung injury in rats. *J Heart Lung Transplant*. 2018;37(6):782–791. doi:10.1016/j.healun.2017.10.025
39. Xia LX, Xiao YY, Jiang WJ, et al. Exosomes derived from induced cardiopulmonary progenitor cells alleviate acute lung injury in mice. *Acta Pharmacol Sin*. 2024;45(8):1644–1659. doi:10.1038/s41401-024-01253-4
40. Chen CM, Chen YJ, Huang ZH. Intratracheal instillation of stem cells in term neonatal rats. *J Vis Exp*. 2020;159:e61117.
41. Fu T, Tian H, Rong H, Ai P, Li X. LncRNA PVT1 induces apoptosis and inflammatory response of bronchial epithelial cells by regulating miR-30b-5p/BCL2L11 axis in COPD. *Genes Environ*. 2023;45(1):24. doi:10.1186/s41021-023-00283-4
42. Izzotti A, Calin GA, Arrigo P, Steele VE, Croce CM, De, Flora S. Downregulation of microRNA expression in the lungs of rats exposed to cigarette smoke. *FASEB J*. 2009;23(3):806–812. doi:10.1096/fj.08-121384
43. Wu T, Tian Q, Liu R, et al. Inhibitory role of bone marrow mesenchymal stem cells-derived exosome in non-small-cell lung cancer: microRNA-30b-5p, EZH2 and PI3K/AKT pathway. *J Cell Mol Med*. 2023;27(22):3526–3538. doi:10.1111/jcmm.17933
44. Zhao J, Li X, Hu J, et al. Mesenchymal stromal cell-derived exosomes attenuate myocardial ischaemia-reperfusion injury through miR-182-regulated macrophage polarization. *Cardiovasc Res*. 2019;115(7):1205–1216. doi:10.1093/cvr/cvz040
45. Lee C, Mitsialis SA, Aslam M, et al. Exosomes mediate the cytoprotective action of mesenchymal stromal cells on hypoxia-induced pulmonary hypertension. *Circulation*. 2012;126(22):2601–2611. doi:10.1161/CIRCULATIONAHA.112.114173
46. Zhu L, Shi Y, Liu L, Wang H, Shen P, Yang H. Mesenchymal stem cells-derived exosomes ameliorate nucleus pulposus cells apoptosis via delivering miR-142-3p: therapeutic potential for intervertebral disc degenerative diseases. *Cell Cycle*. 2020;19(14):1727–1739. doi:10.1080/15384101.2020.1769301